

Figure 2. Riplet and TRIM25 ubiquitin ligases associate with RIG-I. (A, B) HeLa cells were transfected with Riplet-HA expression vector (A) or FLAG-Riplet and TRIM25-HA (B). 24 hours after transfection, the cells were infected with VSV at MOI=1 for six hours. The cells were fixed and stained with anti-RIG-I (Alme-1), HA, and/or FLAG antibodies as indicated. Histograms display the measured fluorescence intensity along the white line in the merged panels. (C–F) Colocalization coefficients of Riplet localization to RIG-I (C) or TRIM25 (E) in mock or VSV infected HeLa cells. Pearson's correlation coefficient of Riplet and RIG-I (D) and TRIM25 (F) (mean \pm SD, $n > 10$). (G, H) HeLa cells were transfected with Riplet-HA (G) or TRIM25-HA (H) expression vector. The cells were stimulated with 100 ng of short poly(I:C) for six hours. The cells were fixed and stained with anti-G3BP and HA antibodies. Colocalization coefficient indicates values (mean \pm SD, $n > 10$) of Riplet (G) or TRIM25 (H) localization to G3BP staining region. Histograms display the measured fluorescence intensity along the white line in the merged panels. (I, J) TRIM25 (I) or Riplet (J) expression vector was transfected into HEK293FT cells together with FLAG-tagged-RIG-I CARDs or -RIG-I RD expression vectors. Cell lysate was prepared at 24 hours after transfection, followed by immunoprecipitation with an anti-FLAG antibody. (K) Riplet, RIG-I, and/or RIG-I- Δ RD, which lacks RD, expression vector was transfected into HEK293 cell with p125luc reporter. Reporter activation was determined at 24 hours after transfection. Data are presented as mean \pm SD ($n = 3$). doi:10.1371/journal.ppat.1003533.g002

mutations reduced the RIG-I polyubiquitination (Figure 4E). RIG-I polyubiquitination in cells stimulated with HCV dsRNA was also reduced by the K788R mutation (Figure 4F). Lys-788 is located within the 55-amino acid region (747–801 aa) of RIG-I essential for RD autorepression of CARDs signaling [31] (Figure 4A). It is possible that the reduction of RIG-I ubiquitination by the mutations was caused by the defect of RIG-I other functions, such as RNA binding activity. However, Figure 3C showed that the RIG-I 5KR and K788R mutant proteins efficiently bound to dsRNA as wild-type RIG-I. This data weakened the above possibility.

Using the RIG-I mutants, we investigated whether Riplet releases RIG-I RD autorepression. Because Riplet ectopic expression activated full-length RIG-I signaling even in the absence of stimulation (Figure 1D), we could assess whether Riplet can remove RIG-I RD autorepression by Riplet ectopic expression study. Due to autorepression, full-length RIG-I expression weakly activates the signaling compared with RIG-I CARDs expression [31]. Riplet ectopic expression increased full-length RIG-I signaling to a level comparable to that of RIG-I CARDs signaling (Figure 5A), suggesting that Riplet released the autorepression. Moreover, the K788R substitution canceled this Riplet ectopic expression effect on RIG-I signaling (Figure 5A). This suggested that the K788R mutation abrogated the release of RIG-I RD autorepression but not RNA binding activity.

Expression of the RIG-I RD fragment is known to represses full-length RIG-I-mediated signaling [3]. Interestingly, Riplet ectopic expression removed the RD fragment repression effect on RIG-I signaling (Figure 5B). This Riplet expression effect was canceled by the K788R amino acid substitution within full-length RIG-I (Figure 5B).

MDA5 C-terminal region does not function as an RD, and thus ectopically expressed MDA5 induced IFN- β promoter activity irrespective of viral infection [3]. If Riplet ectopic expression released RIG-I RD autorepression, it is expected that RIG-I and Riplet co-expression will induce IFN- β promoter activity irrespective of viral infection. As expected, Riplet and RIG-I co-expression induced IFN- β promoter activity irrespective of SeV infection (Figure 5C). Taken together, these genetic data indicated that Riplet released RIG-I RD autorepression.

If Riplet is essential for the release of RIG-I RD autorepression, it is expected that Riplet expression will increase the interaction between RIG-I and TRIM25, because TRIM25 efficiently activated RIG-I CARDs but not full-length RIG-I (Figure 1C and 1D). To test this possibility, we examined the interaction between TRIM25 and RIG-I in the presence or absence of Riplet ectopic expression and found that Riplet expression increased the interaction between TRIM25 and RIG-I (Figure 5D and 5E). Moreover, this interaction was abolished by the K788R mutation (Figure 5F). These data were also consistent with our model that Riplet affects RIG-I RD autorepression rather than RNA binding activity of RIG-I.

If Riplet is essential for the release of RIG-I RD autorepression leading to the interaction between TRIM25 and RIG-I, it was

expected that Riplet is essential for endogenous RIG-I K63-linked polyubiquitination that is mediated by both Riplet and TRIM25. To test this possibility, we investigated endogenous RIG-I K63-linked polyubiquitination in mouse spleen cells infected with SeV. Endogenous RIG-I K63-linked polyubiquitination was increased after SeV infection in wild-type splenocyte, however knockout of Riplet abrogated the endogenous K63-linked polyubiquitination of RIG-I after SeV infection (Figure 5G). Recently, it was reported that knockdown of Riplet strongly reduced endogenous RIG-I polyubiquitination in response to SeV infection in a mouse cell line Hepa 1.6 [32]. Based on our genetic and biochemical data in Figure 3–5, we concluded that Riplet affects RIG-I RD autorepression rather than the RNA binding activity.

Riplet is required for the formation of a hetero-protein complex of RIG-I, TBK1, and IKK- ϵ

Because Riplet-mediated release of RD autorepression increased the interaction between RIG-I and TRIM25, we investigated whether the release of RD autorepression also increased the interaction of RIG-I with other factors. Interestingly, we found that ectopically expressed IKK- ϵ , TBK1, and NEMO ubiquitin binding region co-immunoprecipitated with RIG-I RD (Figure 6A–6D), and Riplet expression enhanced the physical interactions of RIG-I with TBK1, IKK- ϵ , and the NEMO ubiquitin binding region (Figure 6D–6G). The physical interactions between these proteins were not through IPS-1, as IPS-1 did not co-immunoprecipitate with RIG-I RD (Figure 6B).

Microscopy analysis showed that the RIG-I was co-localized with TBK1 or NEMO in the cytoplasm. (Figures 6H and S2A). RIG-I and TBK1 was detected in the region where there is no mitochondria (Figure 6I), and the colocalization of RIG-I with TBK1 was also detected in the region where there is no mitochondria (yellow stained region in Figure 6J). This was consistent with our immunoprecipitation results that RIG-I RD could bind TBK1 without IPS-1. TBK1 is phosphorylated in its activation loop [33]. Surprisingly, the phosphorylated TBK1 (p-TBK1) foci were exclusively localized on mitochondria (Figure 6K and 6L). Co-localization of RIG-I with p-TBK1 was observed after dsRNA stimulation (Figure S2B and S2C). We next assessed the role of endogenous Riplet in the interaction between RIG-I and TBK1. Immunoprecipitation assay showed that Riplet KO reduced the interaction between endogenous RIG-I and TBK1 in mouse spleen cells during VSV infection, indicating that Riplet promoted the interaction between RIG-I and TBK1 (Figure 6M). These data indicated that the Riplet function increased the interaction of RIG-I with TBK1 as well as TRIM25.

Hepatitis C virus protease NS3-4A targets the Riplet protein

Several viruses have evolved strategies to escape the innate immunity. For instance, NS1 of influenza A virus inhibits TRIM25 function. This emphasizes the vital role of TRIM25 in

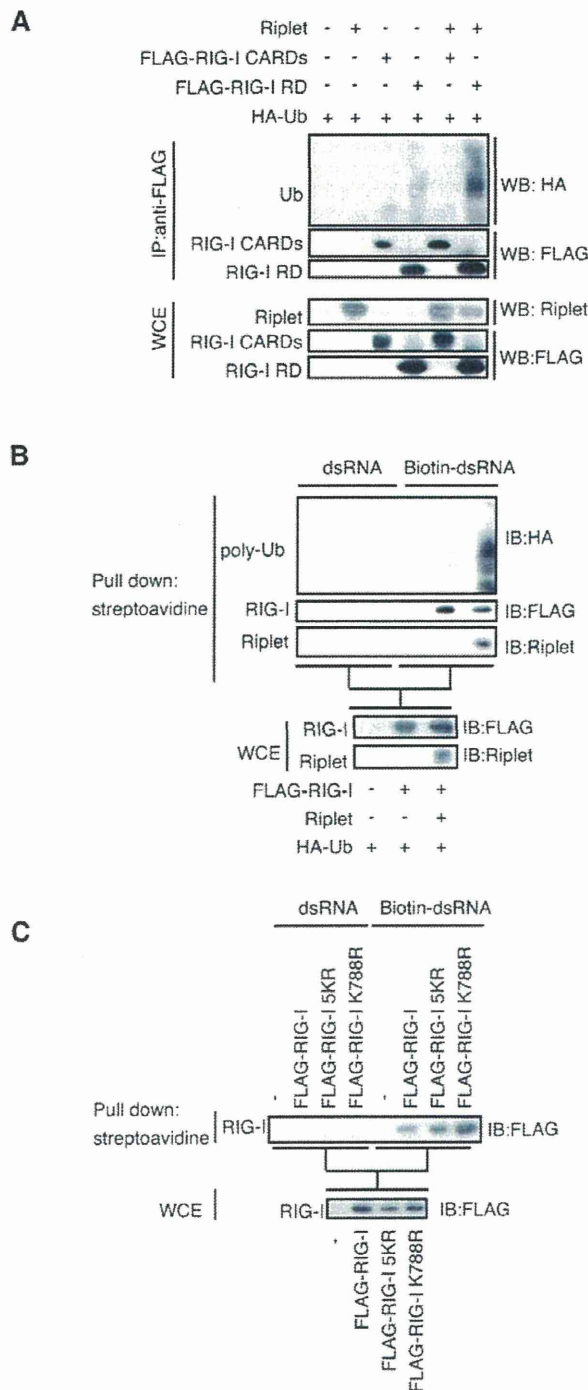


Figure 3. Riplet function is dispensable for RIG-I RNA binding activity. (A) Expression vectors encoding Riplet, FLAG-tagged RIG-I CARDS, and/or FLAG-tagged RIG-I RD were transfected into HEK293FT cells together with an HA-tagged ubiquitin expression vector. Cell lysate was prepared at 24 hours after transfection, followed by immunoprecipitation with an anti-FLAG (RIG-I) antibody. (B) HEK293FT cells were transfected with expression vectors encoding FLAG-tagged RIG-I, Riplet, and HA-tagged ubiquitin. Cell lysate was prepared at 24 hours after transfection, and then incubated with biotin-conjugated (Biotin-dsRNA) or non-conjugated (dsRNA) double-stranded RNA. Biotin-dsRNA was pull-downed with streptavidin beads. Samples were

subjected to SDS-PAGE, and proteins were detected by western blotting. (C) HEK293FT cells were transfected with FLAG-tagged wild-type RIG-I, RIG-I 5KR, or RIG-I K788R expression vector. 24 hours after the transfection, the cell lysate was prepared. The pull down assay with biotin-dsRNA was performed as described above.
doi:10.1371/journal.ppat.1003533.g003

modulating antiviral response [34]. To assess the biological significance of Riplet-mediated release of RIG-I RD autorepression in antiviral innate immune response, we investigated whether viral protein suppresses this mechanism.

The endogenous Riplet protein level was not affected by polyI:C, HCV dsRNA stimulations, or by VSV infection (Figure 7A–7C), however the Riplet protein level was severely reduced in a human hepatocyte cell line with HCV 1b full-length replicons (O cells) compared with hepatocyte cell line without these replicons (O curred cells: Oc cells; Figure 7D), suggesting that viral protein reduced the Riplet protein level. Riplet knockout abolished the expression of type I IFN, IP-10, and type III IFN in response to HCV RNA (Figure 7E), indicating that Riplet was essential for type I IFNs expression in response to HCV RNA.

Because HCV protease NS3-4A suppresses type I IFN expression in response to viral infection [7,25], we examined whether NS3-4A could cleave the Riplet protein. N-terminal FLAG-tagged Riplet or C-terminal HA-tagged Riplet was expressed with or without NS3-4A, after which the Riplet protein levels were compared. NS3-4A expression severely reduced the FLAG-tagged and HA-tagged Riplet protein level but not that of FLAG-tagged RIG-I, whereas catalytically inactive NS3-4A* (S139A) failed to reduce the Riplet protein level (Figure 7F, 7G, and S3A). This suggested that this protease's activity reduced the Riplet protein level. Although NS3-4A reduced IPS-1 protein level as previously reported, NS3-4A did not reduce the TRIM25 and IKK- ϵ protein levels (Figure 7H, 7I, S3B–D).

Within the Riplet RING-finger domain is a sequence that is similar to the NS3-4A target consensus sequence (D/E-x-x-x-x-C/T-S/A; Figure 7J) [35]. NS3-4A cleaves the target just after C/T within this consensus sequence. Acidic amino acids before the C/T site are conserved among the NS3-4A cleavage site within HCV polypeptide. The acidic amino acids from 16 to 18 aa within the Riplet sequence were substituted with Ala, and a Riplet-3A mutant protein was constructed (Figure 7J). The Riplet-3A mutant protein was resistant to NS3-4A (Figure 7I and 7K). Moreover, the Riplet-3A protein co-localized with NS3-4A in cytoplasm (Figure 7L). Interestingly, recombinant NS3-4A that was purified from *E. coli* cleaved the immunoprecipitated FLAG-tagged Riplet protein and recombinant GST-fused Riplet protein purified from *E. coli*, and the cleaved fragments were detected at expected size (Figure 7M and 7N). These data indicated that NS3-4A directly targeted the Riplet protein.

Although Riplet digestion products were not observed in HEK293 cell lysate (Figure S3E and S3F), it is known that the digestion products of TICAM-1 (TRIF) obtained by NS3-4A are not detectable because these products are unstable [28]. Cys-21 of Riplet corresponds to the C/T site in the NS3-4A target consensus sequence. The Cys-21 residue is the first Cys in the RING-finger motif; thus a C21A substitution causes the disruption of RING finger domain structure [36]. The Riplet-C21A mutant protein was unstable and barely detectable (Figure S3G), which suggested that the loss of Cys-21 destabilized the Riplet protein.

HCV protease NS3-4A abolishes an early step of RIG-I activation

To determine if NS3-4A abolishes RIG-I activation by disrupting Riplet, we examined RIG-I ubiquitination and

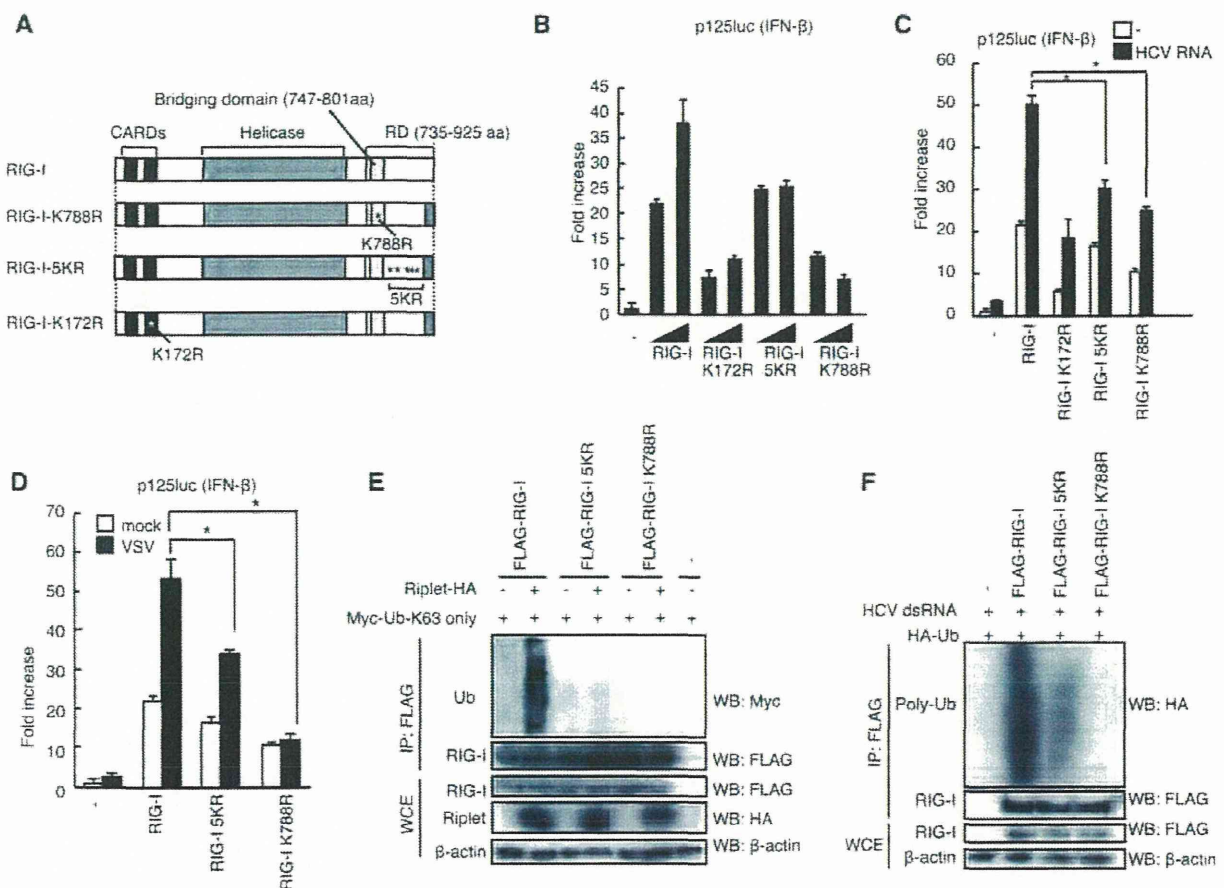


Figure 4. Lys residues within RIG-I RD were essential for Riplet-mediated K63-linked polyubiquitination. (A) Schematic diagram of RIG-I mutant proteins. (B–D) IFN- β promoter activation was determined using a p125luc IFN- β reporter gene. HEK293 cells were transfected with 0.1 μ g of expression vectors encoding full-length RIG-I, RIG-I K172R, RIG-I 5KR, and RIG-I K788R in 24-well plate. The transfected cells were stimulated with 0.1 μ g of HCV 3' UTR dsRNA using lipofectamine 2000 reagent for eight hours (C) or infected with VSV at MOI=1 for 24 hours (D), after which reporter activation was determined. Data are presented as mean \pm SD (n=3). *p<0.05. (E) The expression vectors encoding HA-tagged Riplet and FLAG-tagged RIG-I, RIG-I 5KR, and RIG-I K788R were transfected into HEK293FT cells together with Myc-tagged K63-only ubiquitin expression vector, in which all Lys residues except Lys-63 within ubiquitin were replaced with Arg. At 24 hours after transfection, cell lysates were prepared, followed by immunoprecipitation with an anti-FLAG (RIG-I) antibody. (F) The expression vectors encoding FLAG-tagged wild-type and mutant RIG-I proteins were transfected into HEK293FT cells together with HA-tagged ubiquitin expression vector. 24 hours after the transfection, the cells were stimulated with HCV 3' UTR dsRNA by transfection for eight hours. Then cell lysate was prepared and immunoprecipitation was performed with anti-FLAG antibody. doi:10.1371/journal.ppat.1003533.g004

interaction between RIG-I and TRIM25. Riplet-mediated ubiquitination of full-length RIG-I or RIG-I RD was abolished by NS3-4A expression (Figure 8A and 8B). K63-linked polyubiquitination of RIG-I RD in SeV infected cells were also reduced by NS3-4A expression (Figure 8C). Moreover, NS3-4A expression reduced the interaction between TRIM25 and full-length RIG-I (Figure 8D).

An IPS-1-C508A mutant protein is resistant to NS3-4A cleavage [7]. A reporter gene assay showed that NS3-4A expression severely reduced IFN- β promoter activation induced by RIG-I and Riplet expression even in the presence of the IPS-1 C508A mutant protein in HEK293 cell (Figure 9A), and a catalytically inactive NS3-4A mutant failed to reduce this signal (Figure 9B). These data were consistent with our observation that NS3-4A targeted the Riplet protein. There was endogenous IPS-1 in HEK293 cell, and thus the decrease of IFN- β promoter induction by NS3-4A in HEK293 cell could be due to the cleavage of endogenous IPS-1 by NS3-4A. To exclude this possibility, we

next used IPS-1 KO mouse hepatocyte [37]. The IPS-1 C508A mutant protein was expressed in IPS-1 KO hepatocyte. NS3-4A expression reduced the reporter activation induced by RIG-I/Riplet expression or by stimulation with HCV dsRNA even in the presence of IPS-1 C508A (Figure 9C and 9D). These results indicated that NS3-4A targeted both IPS-1 and upstream factors of IPS-1 and were consistent with our observation that NS3-4A reduced the Riplet protein level. We could not test whether NS3-4A failed to impair IFN- β promoter activity in the presence of the Riplet-3A and Riplet C21A mutants because the mutant proteins were not functional and failed to activate RIG-I (Supplemental Figure S3H and S3I). Thus, we could not exclude the possibility that NS3-4A targeted another protein in addition to Riplet and IPS-1.

Hepatitis C virus abrogates endogenous Riplet function

Endogenous RIG-I exhibited punctate staining in the human hepatocyte cell line HuH7 and HepG2 cells after stimulation with

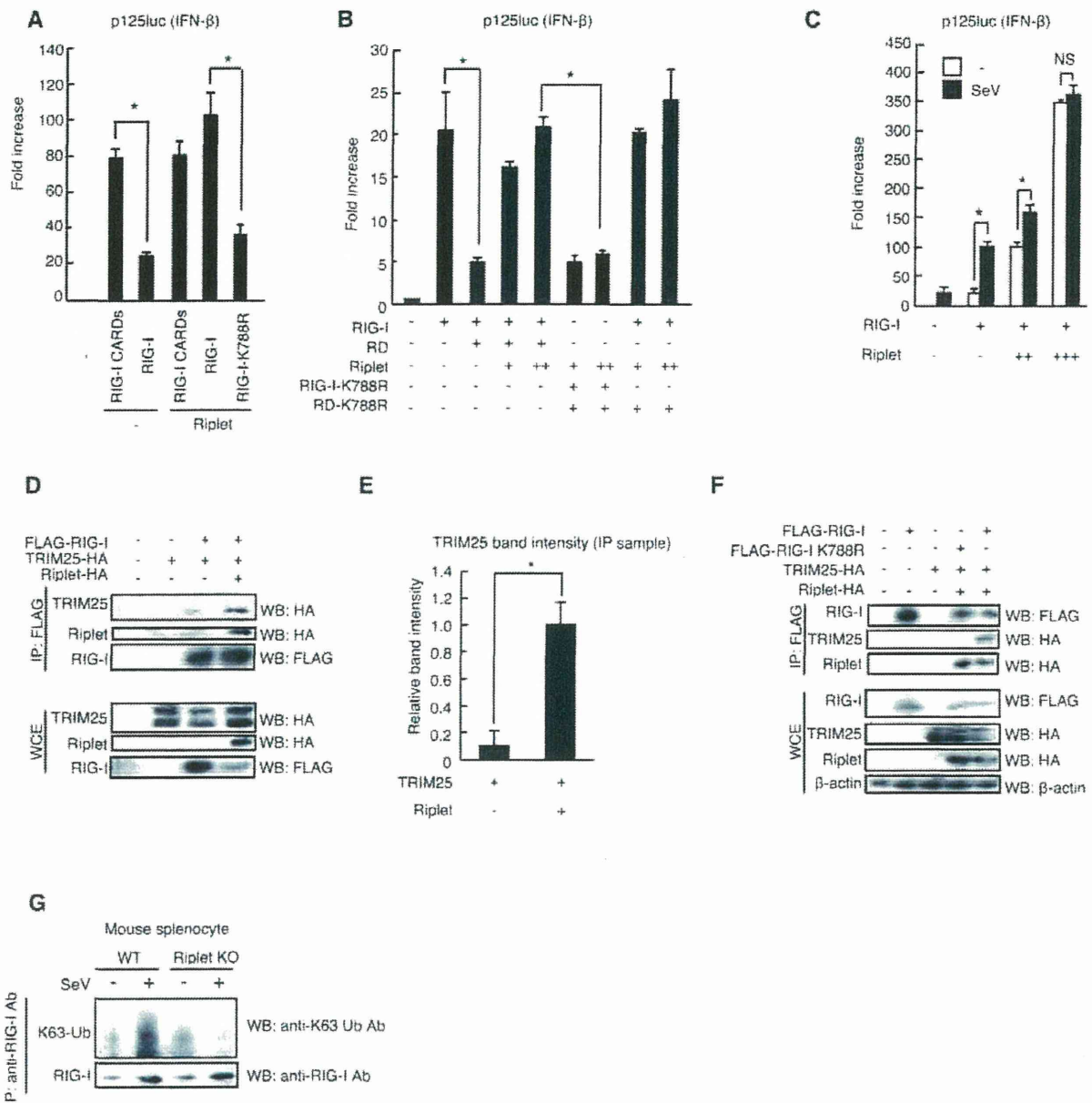
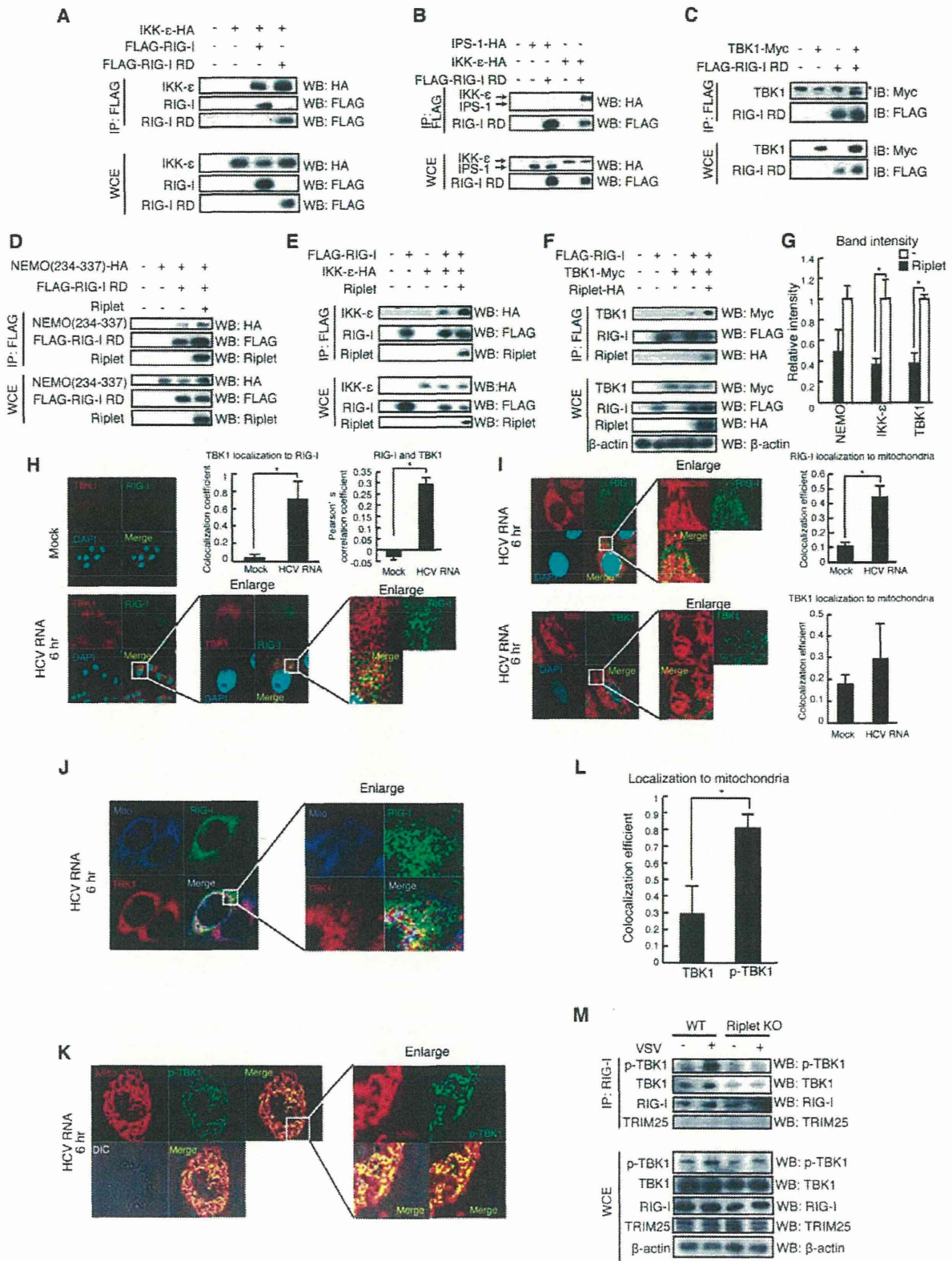


Figure 5. Riplet affects RIG-I RD autorepression of CARDs signaling. (A, B) IFN- β promoter activation was determined using a p125luc IFN- β reporter gene. Expression vectors encoding RIG-I CARDs, full-length RIG-I, RIG-I K788R, RD, RD-K788, and/or Riplet were transfected into HEK293 cells as indicated. Reporter activation was determined after transfection. Data are presented as mean \pm SD (n = 3). *p < 0.05. (C) IFN- β promoter activation was determined using a p125luc IFN- β reporter gene. RIG-I and Riplet expression vectors were transfected into HEK293 cells as indicated. 24 hours after transfection, cells were infected with SeV at MOI = 1 for 24 hours, and the reporter activities were determined. (D–F) HEK293FT cells were transfected with expression vectors encoding FLAG-tagged RIG-I, HA-tagged TRIM25, HA-tagged Riplet, FLAG-tagged RIG-I K788R as indicated. Cell lysate was prepared at 24 hours after transfection, followed by immunoprecipitation with an anti-FLAG antibody (RIG-I). Relative band intensity of immunoprecipitated TRIM25 in panel D was determined (E). (G) Mouse splenocyte was isolated from wild-type and Riplet KO mice spleen. The cells were infected with SeV, and then cell lysate was prepared. Immunoprecipitation was carried out with anti-RIG-I rabbit mAb (D14G6), and subjected to SDS-PAGE. Endogenous K63-linked polyubiquitin chain was detected using K63-linked polyubiquitin chain specific antibody.
doi:10.1371/journal.ppat.1003533.g005

HCV RNA (Figure 9E) but not in HuH7.5 cell line (Figure 9E). In HuH7.5 cells, there is a T55I mutation within endogenous *RIG-I* gene that disrupts the interaction between RIG-I and TRIM25 [38]. We investigated whether Riplet is required for RIG-I to exhibit punctate staining, and found that knockdown of Riplet

decreased RIG-I punctate staining induced by HCV RNA (Supplemental Figure S4). We next investigated whether HCV abrogated Riplet-dependent RIG-I punctate pattern in the cytoplasm. As expected, RIG-I failed to exhibit punctate staining in O cells with HCV replicons in NS3 positive cells and HuH7



Mouse splenocyte

Figure 6. The association of TBK1 and IKK- ϵ protein kinases with RIG-I RD is enhanced by Riplet. (A–F) The interaction of RIG-I with TBK1, IKK- ϵ , and NEMO was examined by immunoprecipitation assay. FLAG-tagged RIG-I or RIG-I RD expression vector was transfected into HEK293FT cells together with HA-tagged IKK- ϵ (A, B, and E), Myc-tagged TBK1 (C, F), HA-tagged NEMO ubiquitin binding region (D), and/or Riplet (D–F) expression vectors as indicated. 24 hours after the transfection, cell lysate was prepared, and immunoprecipitation was performed with anti-FLAG antibody. Asterisk indicates non-specific bands. (G) Relative band intensity of immunoprecipitated NEMO, IKK- ϵ , and TBK1 in D–F was determined. (H–L) Intracellular localization of endogenous RIG-I (H–J), TBK1 (H–J), phosphorylated-TBK1 (p-TBK1) (K), and mitochondria (I–K) were observed using anti-RIG-I (Alme-1), TBK1, p-TBK1 mAbs, and mitotracker. HeLa cells were stimulated with HCV dsRNA for six hours using lipofectamine 2000. Colocalization coefficient of TBK1 localization to RIG-I (H), RIG-I and TBK1 localization to mitochondria (I), and TBK1 and p-TBK1 localization to mitochondria (L) were determined (mean \pm sd, $n > 10$). Person's correlation coefficient of RIG-I and TBK1 was determined (H). (M) Splenocytes from wild type and Riplet KO mouse were infected with VSV at MOI = 10 for eight hours. Immunoprecipitation was performed using an anti-RIG-I rabbit monoclonal antibody (D14G6), and the immunoprecipitates were analyzed by SDS-PAGE. Endogenous RIG-I, TBK1, TRIM25, and β -actin were detected using anti-RIG-I, p-TBK1, TRIM25, and β -actin antibodies.
doi:10.1371/journal.ppat.1003533.g006

cells infected with HCV JFH1 (Figure 9F–9H). We confirmed that HCV disrupted IPS-1 in our experimental condition (Figure 9G and 9H).

To further assess whether HCV abrogates endogenous Riplet function, we observed endogenous K63-linked polyubiquitination of RIG-I in cells with HCV replicons. Although SeV infection induced endogenous K63-linked polyubiquitination of RIG-I in HuH7 cells, HCV replicons failed to increase the polyubiquitination (Figure 9I). Next, we investigated the association of endogenous RIG-I with TRIM25 and TBK1, which is promoted by Riplet as shown in Figure 5 and 6. SeV infection induced the association of endogenous RIG-I with TRIM25 and TBK1, whereas HCV replicons failed to induce the association (Figure 9J). Taken together, these data indicated that HCV abrogated endogenous Riplet function.

Although NS3-4A cleaves IPS-1, a mutation within endogenous RIG-I gene increased the permissiveness to HCV infection in HuH7-derived cells [3], indicating that RIG-I is required for antiviral response to HCV infection before NS3-4A cleaves IPS-1. We used siRNA to knockdown endogenous Riplet in HuH7 cells, and then the cells were infected with HCV JFH1. Interestingly, Riplet knockdown increased the permissiveness to HCV JFH1 infection (Figure 9K), indicating that endogenous Riplet is required for antiviral response to HCV infection.

Discussion

RIG-I activation is regulated by two ubiquitin ligases Riplet and TRIM25 [15,21]. The two ubiquitin ligases are essential for RIG-I activation [15,23], however the functional difference had been unclear. It is known that TRIM25 is essential for RIG-I oligomerization and association with IPS-1 adaptor molecule [15,19]. Here, we demonstrated that Riplet was essential for the release of RIG-I RD autorepression of its CARDs, which resulted in the association with TRIM25. This functional difference explained the reason why RIG-I requires the two ubiquitin ligases for triggering the signal.

It has been reported that TRIM25 activates RIG-I signaling [15,19]. We confirmed that ectopic expression of TRIM25 increases RIG-I CARDs-mediated signaling. However, most previous studies used a RIG-I CARDs fragment but not full-length RIG-I [15,19,38]. Unexpectedly, we found that the increase of full-length RIG-I-mediated signaling by TRIM25 expression was much less than that of the CARDs-mediated signaling. It is intriguing that Riplet helped TRIM25 to activate full-length RIG-I. Riplet expression promoted the interaction between TRIM25 and full-length RIG-I, and this interaction was abrogated by a RIG-I K788R mutation, which reduced Riplet-mediated RIG-I ubiquitination. Thus, we propose that Riplet-mediated polyubiquitination of RIG-I RD is a prerequisite for TRIM25 to activate RIG-I (Figure 10).

Ectopic expression of Riplet activated RIG-I without stimulation with RIG-I ligand. This is not surprising because ectopically expressed Riplet bound to RIG-I without stimulation with RIG-I ligand, whereas endogenous Riplet bound to endogenous RIG-I after stimulation with RIG-I ligand. RIG-I undergoes its conformational change after binding to a ligand [3,39]. The conformational change would allow the access of endogenous Riplet to RIG-I, which resulted in Riplet-mediated K63-linked polyubiquitination leading to the release of RD autorepression. This model is consistent with the observation that TRIM25 ectopic expression did not activate full-length RIG-I without Riplet expression, because TRIM25 hardly bound to full-length RIG-I without Riplet.

Previously, we reported that the five Lys residues within RIG-I RD were important for Riplet-mediated RIG-I ubiquitination. We constructed the RIG-I 5KR mutant and indicated that the 5KR mutation reduced RIG-I ubiquitination and activation without loss of RNA binding activity. This is consistent with our previous conclusion. However, there is residual ubiquitination of RIG-I 5KR mutation, and we found that K788R mutation showed more severe phenotype. These data indicated that Riplet targeted the several Lys residues within RIG-I RD. This is not surprising, because TRIM25 targets not only Lys-172 but also other Lys residues within mouse RIG-I CARDs [32].

TBK1 and IKK- ϵ are downstream factors of IPS-1. We found that TBK1 and IKK- ϵ could bind RIG-I RD. It is possible that RIG-I associates with TBK1 through IPS-1. However, Hiscott J and colleagues demonstrated that IKK- ϵ could bind IPS-1 and that TBK1 did not bind IPS-1 [40]. Moreover, RIG-I RD did not bind IPS-1, and RIG-I and TBK1 co-localization was detected in the cytoplasmic region where there are no mitochondria. These observations weaken this possibility. Our results indicated that RIG-I RD bound to the NEMO ubiquitin binding region. IRF-3 activation requires the ubiquitin binding domain of NEMO, and an endogenous K63-linked polyubiquitin chain plays a key role in IRF3 activation [41]. Thus, we prefer a model in which TBK1 associates with an RIG-I RD-anchored polyubiquitin chain through NEMO (Figure 10). Although Riplet knockout reduced the binding of RIG-I to TBK1, residual binding was still detectable. Thus, there appears to be Riplet-dependent and independent associations between RIG-I and TBK1. TRAF3 is an E3 ubiquitin ligase, and is involved in the RIG-I-mediated type I IFN production pathway [42]. Because there is residual activation of the type I IFN production pathway even in TRAF3 knockout cells [41], it is possible that the RIG-I polyubiquitin chain may compensate for the TRAF3 defect in recruiting TBK1 to mitochondria. Further studies will be needed to determine the precise molecular mechanisms. Although TBK1 dispersed in the cytoplasm, p-TBK1 was exclusively localized on mitochondria. Considering that TBK1 is phosphorylated in its activation loop [33], these results suggested that RIG-I RD associated with

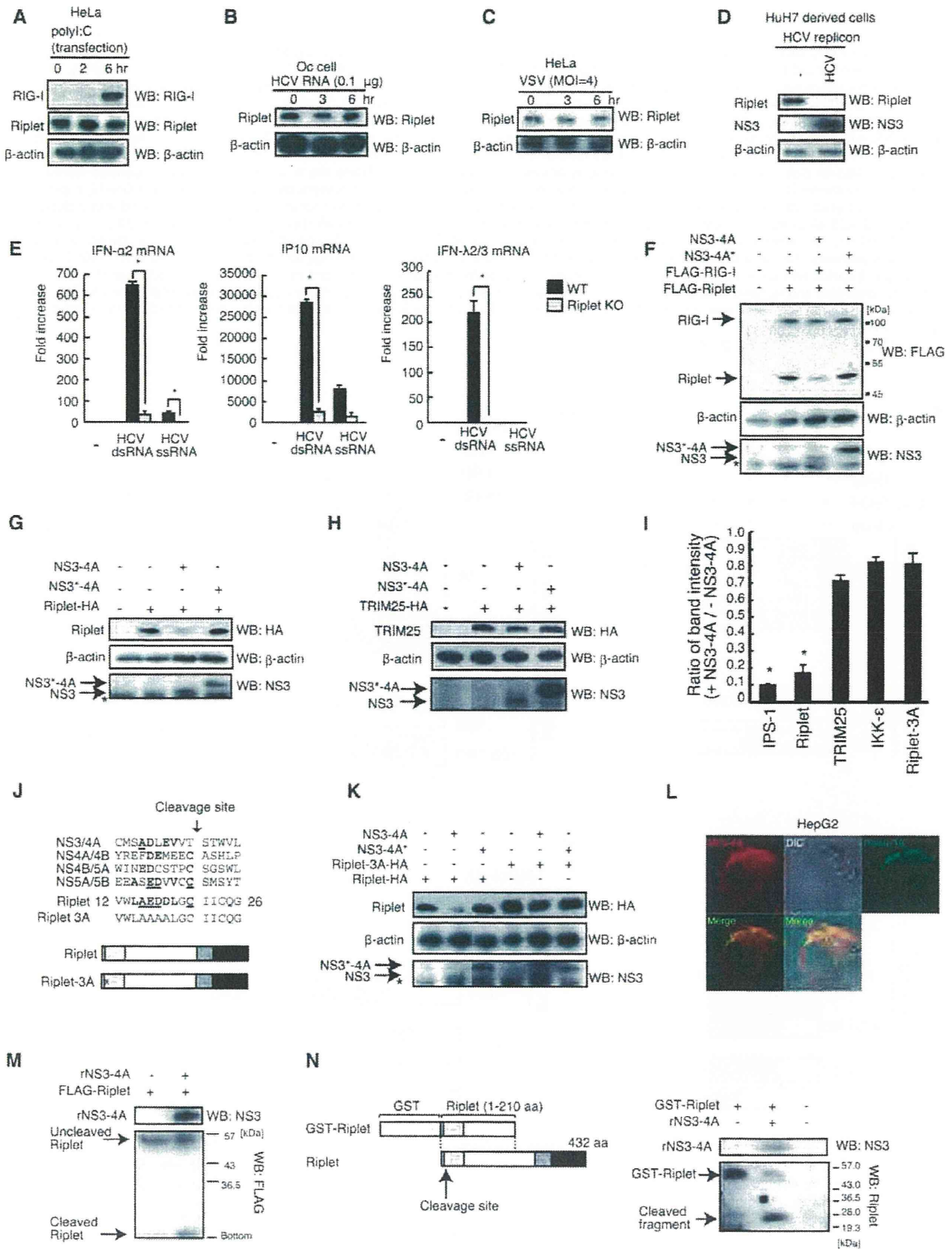


Figure 7. NS3-4A of HCV targets the Riplet protein. (A–D) Endogenous RIG-I and Riplet protein levels were observed by western blotting. HeLa cells were stimulated with polyI:C transfection (A), HCV dsRNA transfection (B) or infected with VSV (C). HCV replicon positive (HCV) and negative (-) cell lysates were prepared from a HuH7-derived cell line O cell that contains HCV 1b full-length replicons and O curred cell (Oc cell) in which HCV replicons were removed by IFN treatment (D). (E) The response to HCV RNA in wild-type and Riplet KO MEFs was examined by RT-qPCR. Wild type (WT) and Riplet knockout (KO) MEF cells were transfected with 100 ng of HCV ssRNA and dsRNA. Six hours after stimulation, mRNA expressions of IFN- α 2, IP10, and IFN- λ 2/3 were measured by RT-qPCR. Data are presented as mean \pm SD (n=3). *p<0.05. (F–H) FLAG-tagged Riplet and RIG-I (F), HA-tagged Riplet (G), or HA-tagged TRIM25 (H) expression vectors were transfected into HEK293FT cells together with NS3-4A or NS3-4A* expression vectors. NS3-4A* mutant protein harbors an amino acids substitution at its catalytic site Ser-139 with Ala. 24 hours after transfection, cell lysate was prepared and subjected to SDS-PAGE. (I) Band intensity ratio of IPS-1, Riplet, TRIM25, IKK- ϵ , and Riplet-3A with/without NS3-4A expression (mean \pm sd, n=3). (J) NS3-4A cleavage sites within an HCV polypeptide are compared with a candidate site in the Riplet RING-finger domain. Homologous amino acids are shown in bold, and identical amino acids are underlined. In Riplet-3A mutant protein, three acidic amino acids, Glu-16, Asp-17, Asp-18, were substituted with Ala. (K) An expression vector encoding wild-type Riplet or Riplet-3A mutant protein was transfected into HEK293 cells together with NS3-4A or NS3-4A* expression vectors. Cell lysate was prepared 24 hours after transfection, and subjected to SDS-PAGE. (L) HA-tagged Riplet-3A and NS3-4A expression vectors were transfected into HepG2 cell. 24 hours after transfection, the cells were fixed and stained with anti-HA monoclonal antibody (mouse) and anti-NS3-4A polyclonal antibody (goat). (M) N-terminal FLAG-tagged Riplet was expressed in HEK293FT cells, and immunoprecipitation was carried out with anti-FLAG antibody. Immunoprecipitates were incubated with recombinant NS3-4A purified from *E.coli* at 37°C for one hour, and samples were subjected to SDS-PAGE analysis. The proteins were detected by western blotting. (N) Purified GST fused Riplet (1–210 aa) was incubated with or without recombinant NS3-4A (rNS3-4A) at 37°C for 30 min. The proteins were subjected to SDS-PAGE and detected by western blotting.

doi:10.1371/journal.ppat.1003533.g007

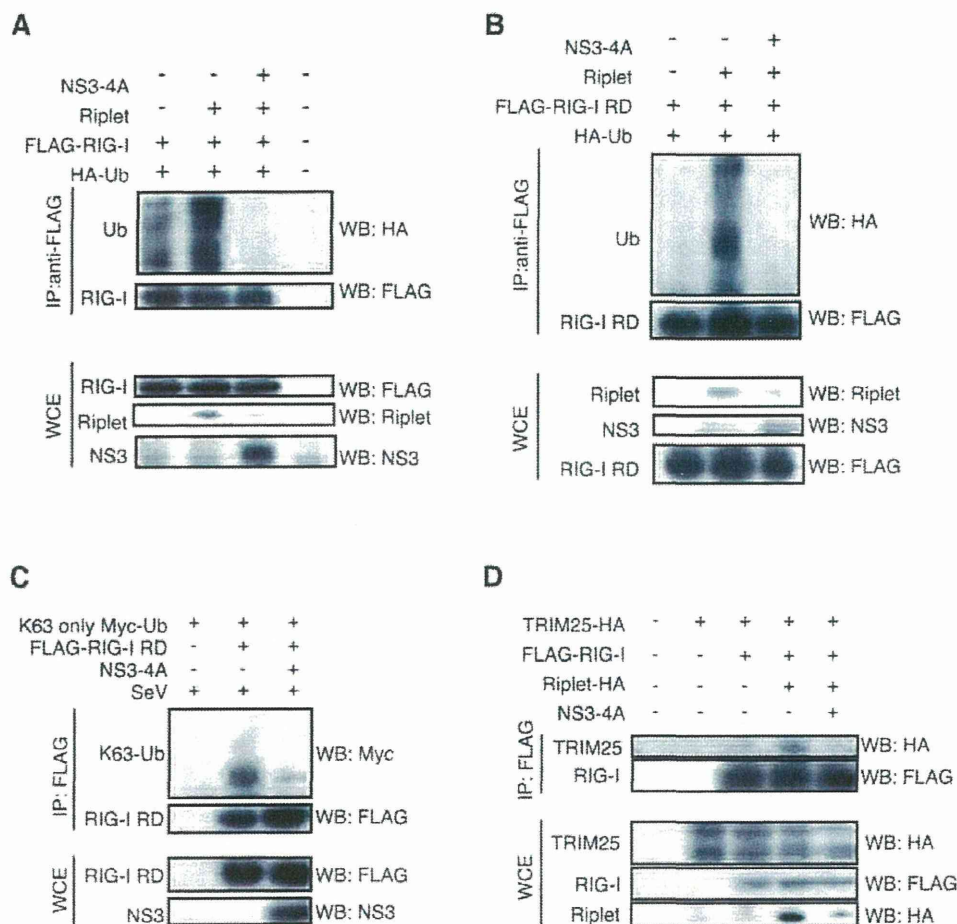


Figure 8. NS3-4A inhibits Riplet-mediated RIG-I polyubiquitination. (A, B) Riplet, NS3-4A, and/or HA-tagged ubiquitin (HA-Ub) expression vectors were transfected into HEK293FT cells along with either full-length RIG-I (A) or RIG-I RD (B). Cell lysate was prepared 24 hours after transfection, and subjected to SDS-PAGE. The proteins were detected by western blotting. (C). HEK293FT cells were transfected with Myc-tagged K63-only ubiquitin, FLAG-tagged RIG-I RD, and/or NS3-4A expression vectors. 24 hours after the transfection, cells were infected with SeV for six hours, and then cell lysate was prepared. Immunoprecipitation was carried out with anti-FLAG antibody, and the samples were subjected to SDS-PAGE. (D) HA-tagged TRIM25, Riplet and/or FLAG-tagged RIG-I expression vectors were transfected into HEK293FT cells with or without NS3-4A expression vector. Cell lysate was prepared 24 hours after the transfection, and immunoprecipitation assay was performed with anti-FLAG antibody. The precipitates were subjected to SDS-PAGE.

doi:10.1371/journal.ppat.1003533.g008

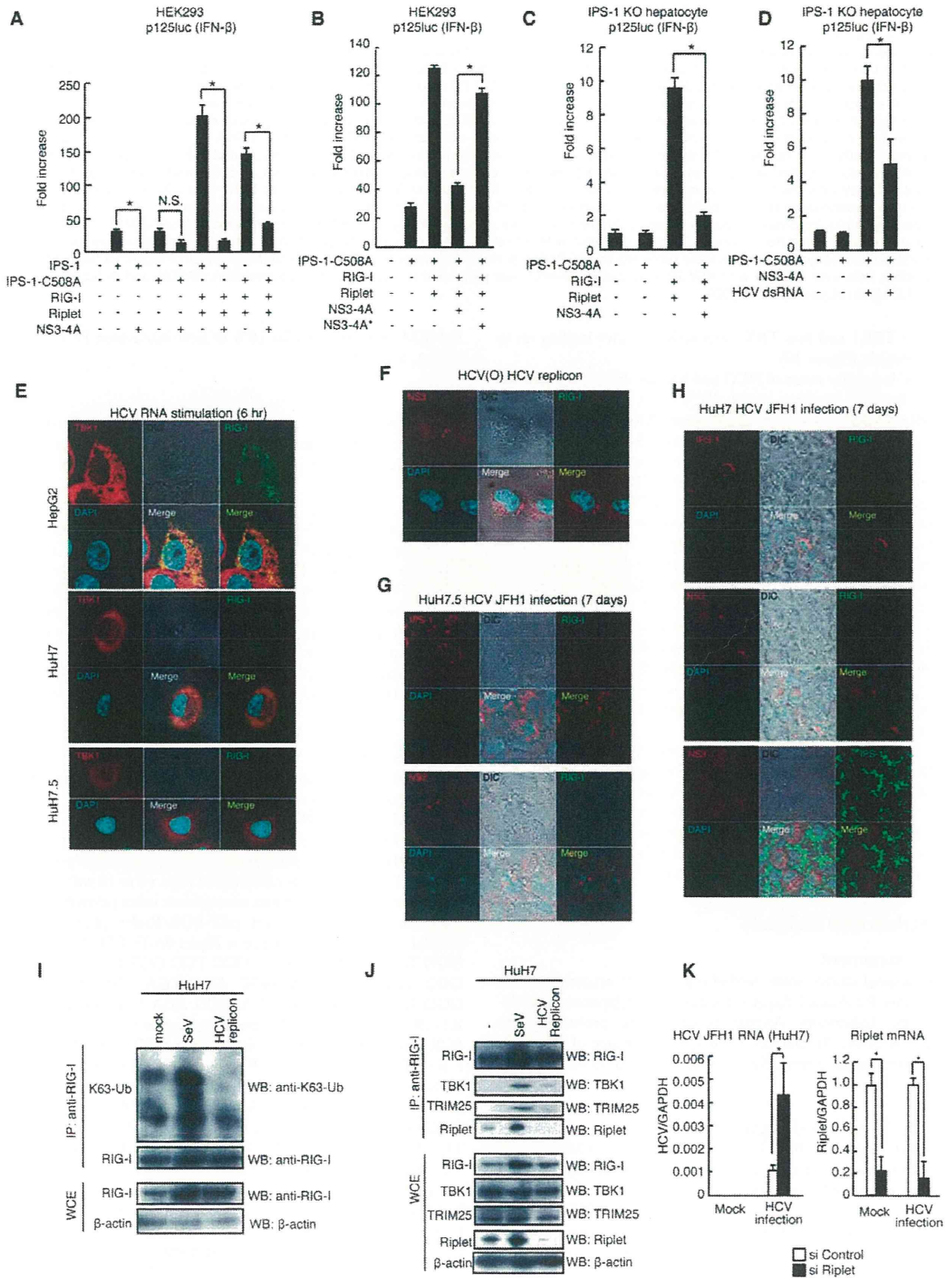


Figure 9. HCV abrogated Riplet-mediated RIG-I activation. (A and B) The inhibition of IFN- β promoter activation by NS3-4A was assessed by reporter gene assays. IPS-1-C508A mutant protein harbors an amino acid substitution at Cys-508 with Ala. 100 ng of IPS-1, IPS-1-C508A, RIG-I, Riplet, NS3-4A, and/or NS3-4A* expression vectors were transfected into HEK293 cells in 24-well plates with p125luc reporter plasmid. The total amount of transfected DNA (800 ng/well) was kept constant by adding empty vector (pEF-BOS). 24 hours after the transfection, the reporter activities were measured. Data are presented as mean \pm SD (n=3). *p<0.05. (C and D) IPS-1 KO mouse hepatocyte was transfected with IPS-1 C508A, RIG-I, Riplet, and/or NS3-4A expression vectors together with p125luc and *Renilla* luciferase plasmids. Transfected cells were stimulated with 50 ng of HCV dsRNA for 24 hours by transfection (D). Data are presented as mean SD (n=3). *p<0.05. (E and F) Intracellular localizations of endogenous TBK1 and RIG-I were determined by confocal microscopy. HepG2, HuH7, and HuH7.5 cells were stimulated with 100 ng of HCV dsRNA for six hours by transfection (E). Stimulated cells (E) and O cells with HCV replicons (F) were stained with anti-RIG-I, TBK1, and/or NS3 antibodies. (G and H) HuH7 (G) and HuH7.5 (H) cells were infected with HCV JFH1 strain. Seven days after the infection, the cells were stained with anti-RIG-I, IPS-1, and NS3 antibodies. (I) HuH7 cells were infected with SeV at MOI=1 for 24 hours. Cell lysates were prepared from mock or SeV infected HuH7 or HuH7 cells with HCV replicons (O cell). Immunoprecipitation using high salt buffer was performed with anti-RIG-I (Alme-1) antibody. The samples were subjected to SDS-PAGE. Endogenous K63-linked polyubiquitin chain was detected using ubiquitin K63-linkage specific antibody. (J) HuH7 cells were infected with SeV at MOI = 1 for 24 hours. Cell lysates were prepared from mock or SeV infected HuH7 or HuH7 cells with HCV replicons (O cell). Immunoprecipitation was performed with anti-RIG-I (Alme-1) antibody. The samples were subjected to SDS-PAGE. (K) HuH7 cells were transfected with siRNA for mock or Riplet. 48 hours after the transfection, cells were infected with HCV JFH1 for 2 days. RT-qPCR was performed to determine HCV genome RNA, GAPDH, and Riplet expression. doi:10.1371/journal.ppat.1003533.g009

inactive TBK1 and that TBK1 was activated after loading on to mitochondria (Figure 10).

HCV is a major cause of HCC and has the ability to evade host innate immune response [7,43]. HCV RNA is primarily recognized by the cytoplasmic viral RNA sensor RIG-I. Previous studies showed that the protease NS3-4A cleaves IPS-1 to shut off RIG-I signaling. However, our results indicated that there was another target of NS3-4A in RIG-I signaling. First, RIG-I failed to exhibit punctate staining in cells infected with HCV. Second, NS3-4A reduced RIG-I signaling even in the presence of an IPS-1-C508A mutant, which is resistant to the cleavage by NS3-4A. Third, the endogenous Riplet protein level was severely reduced in cells with HCV replicons. Fourth, NS3-4A targeted Riplet and abrogated Riplet-dependent RIG-I ubiquitination and complex formation with TRIM25 and TBK1. These data support our model that NS3-4A targets not only IPS-1 but also Riplet to escape host innate immune responses (Figure 10). Recently it was reported that NS1 proteins of Influenza A virus inhibited Riplet function [32]. These findings indicated biological importance of Riplet in RIG-I activation during viral infection.

In general, a ubiquitin ligase has several targets. We have performed yeast two-hybrid screening using Riplet as bait and found a candidate clone that encodes a tumor suppressor gene. Our pilot study showed that Riplet mediated K63-linked polyubiquitination of this tumor suppressor and suppressed retinoblastoma (Rb) activity. Thus, Riplet disruption by NS3-4A might be a cause of liver disease induced by HCV infection.

Materials and Methods

Ethics statement

All animal studies were carried out in strict accordance with Guidelines for Animal Experimentation of the Japanese Association for Laboratory Animal Science. The protocols were approved by the Animal Care and Use Committee of Hokkaido University, Japan (Permit Number: 08-0245 and 09-0215).

Cell

HEK293, Vero, and HepG2 cells were cultured in Dulbecco's modified Eagle's medium low glucose medium (D-MEM) with 10% heat-inactivated fetal calf serum (FCS) (Invitrogen). HeLa cells were cultured in minimum Eagle's medium with 2 mM L-glutamine and 10% heat-inactivated FCS. HEK293FT cells were maintained in D-MEM high glucose medium containing 10% of heat-inactivated FCS (Invitrogen). Human hepatocyte cell line with HCV 1b full-length replicons (O cells) and O cured cells (Oc cells) were kindly gifted from Kato N [44]. O cells were cultured in

D-MEM high glucose with 10% of heat-inactivated FCS, G418, NEAA, and L-Gln.

Viruses

VSV Indiana strain and SeV HVJ strain were amplified using Vero cells. To determine the virus titer, we performed plaque assay using Vero cells. HCV JFH1 was amplified using HuH7.5 cells.

Mice

Generation of IPS-1 KO and Riplet KO mice were described previously [23,45]. Splenocyte was isolated from C57BL/6 wild-type and Riplet KO mice. Isolated cells were cultured in RPMI1640 containing 10% of heat-inactivated FCS. The preparations of wild-type and Riplet KO MEFs were described previously [23]. Preparation of IPS-1 KO mouse hepatocyte was described previously [37]. All mice were maintained under specific-pathogen free conditions in the animal facility of the Hokkaido University Graduate School of Science (Japan).

Plasmids

Expression vectors encoding for N-terminal FLAG-tagged RIG-I, N-terminal FLAG-tagged RIG-I CARDs (dRIG-I), FLAG-tagged RIG-I Δ RD (RIG-I-dRD), FLAG-tagged RIG-I RD, C-terminal HA-tagged TRIM25, C-terminal HA-tagged Riplet, and Riplet- Δ RING (Riplet-DN) plasmids were described previously [21,23]. The amino acids substitutions from 16 to 18 with Ala was carried out by PCR-mediated mutagenesis using primers, Riplet-3A-F and Riplet-3A-R and pEF-BOS/Riplet plasmid as a template. The primer sequence is Riplet-3A-F: TTC CCG TGT GGC TGG CCG CGG CCG CCC TCG GCT GCA TCA TCT GCC, and Riplet-3A-R: GGC AGA TGA TGC AGC CGA GGG CGG CCG CGG CCA GCC ACA CGG GAA. RIG-I K172R and RIG-I K788R expression vectors were constructed by PCR-mediated mutagenesis using primers, RIG-I K172R-F, RIG-I K172R-R, RIG-I K788R-F and RIG-I-K788R-R, and pEF-BOS/FLAG-RIG-I plasmid as a template. The primer sequences are RIG-I K172R-F: GGA AAA CTG GCC CAA AAC TTT GAG ACT TGC TTT GGA GAA AG, RIG-I K172R-R: CTT TCT CCA AAG CAA GTC TCA AAG TTT TGG GCC AGT TTT CC, RIG-I-K788R-F: TGC ATA TAC AGA CTC ATG AAA GAT TCA TCA GAG ATA GTC AAG AA, and RIG-I-K788R-R: CTT GAC TAT CTC TGA TGA ATC TTT CAT GAG TCT GTA TAT GCA G. RIG-I 5KR expression vectors were constructed by PCR-mediated mutagenesis using primers, RIG-I 849 851 RR-F, RIG-I 849 851 RR-R, RIG-I 888R-F, RIG-I 888R-R, RIG-I 907 909 RR-F, RIG-I 907 909 RR-R, and